nature communications

Article

https://doi.org/10.1038/s41467-026-69190-w

Global patterns of inequality in pedestrian shade provision

Received: 11 September 2025

Accepted: 15 January 2026

Published online: 10 February 2026

Check for updates

Xinyue Gu[1,2] ✉, Lukas Beuster[1,3,4], Xintao Liu[2] ✉, Eveline van Leeuwen[4,5], Titus Venverloo[1,4] & Fábio Duarte[1] ✉

Shade provision is the most effective strategy for mitigating heat in cities; yet its distribution remains highly uneven. Using high-resolution simulations of shade casting from buildings and trees on pedestrian areas, combined with socioeconomic data at the neighbourhood level, we assess shade availability across nine climatically and geographically diverse cities: Amsterdam, Barcelona, Belém, Boston, Hong Kong, Milan, Rio de Janeiro, Stockholm, and Sydney. Our results reveal a consistent pattern of spatial and socioeconomic inequality: lower-income and peripheral neighbourhoods tend to receive significantly less shade on sidewalks, despite facing greater heat vulnerability. Notably, inequality persists even in cities with high overall shade coverage, where wealthier areas benefit from disproportionate abundance. By focusing on public pedestrian spaces, rather than general coverage, this study highlights the importance of measuring heat burden through the lens of human experience. We call for equity-centred adaptation strategies that target shade provision where it is most needed, particularly in underserved and exposed communities.

As global temperatures continue to rise, cities are becoming epicentres of extreme heat exposure, amplifying risks to public health, energy security, and social equity[1,2]. Urban populations are especially vulnerable due to the Urban Heat Island effect, which intensifies the frequency, duration, and severity of heatwaves[3,4]. The consequences are profound, ranging from increased damaged infrastructure[5,6], mortality and morbidity[7], decreased labour productivity[8,9], strained energy systems[10,11], and amplified social and spatial inequalities[12,13]. These impacts disproportionately burden marginalised neighbourhoods, exacerbating existing urban vulnerabilities under climate change.

Urban shade has emerged as a highly effective yet underutilised strategy to mitigate urban heat[14,15]. Trees, buildings, and other shade-producing infrastructure can significantly reduce surface temperatures and thermal radiation exposure, thereby reducing heat-related health risks[16,17]. While both forms of shade reduce direct solar load, tree shade provides additional cooling through evapotranspiration, a biophysical process that lowers air temperature through moisture exchange[18,19]. The relative effectiveness of these mechanisms depends strongly on climatic context: in hot-dry climates, the low ambient humidity enhances the cooling impact of trees, whereas in humid environments, the evaporative potential is constrained[20–22], and shading from built structures may dominate the comfort response.

These cooling benefits have been well documented, demonstrating that shade can reduce the net heat burden by up to 40°C[23–26], substantially improving the thermal comfort of pedestrians and lowering heat stress. However, studies have increasingly revealed that shade is unevenly distributed across socioeconomic lines[14]. For instance, in the United States, the tree canopy in the most impoverished neighbourhoods is 41% lower than in the wealthiest areas, and neighbourhoods of people of colour have one-third less shade than

[1]Senseable City Lab, Massachusetts Institute of Technology, Cambridge, USA. [2]Department of Land Surveying and Geo-Informatics, The Hong Kong Polytechnic University, Hong Kong, China. [3]3D Geoinformation Research Group, Delft University of Technology, Delft, the Netherlands. [4]Amsterdam Institute for Advanced Metropolitan Solutions, Amsterdam, the Netherlands. [5]Urban Economics Group, Wageningen University & Research, Wageningen, the Netherlands. ✉e-mail: xinyue.gu@connect.polyu.hk; xintao.liu@polyu.edu.hk; fduarte@mit.edu

those where white residents are the majority[27,28]. This raises concerns about environmental justice and climate adaptation equity.

Despite the growing recognition of urban shade as a critical component of climate-resilient cities, systematic assessments of its spatial distribution remain scarce[14]. Prior research has predominantly focused on the distribution of green spaces[29–31] or tree canopy cover[32,33], and has largely overlooked how shade provision varies across neighbourhoods. Moreover, most studies are limited to single cities, lacking comparative insights across climatic and cultural contexts[34–36]. While recent advances in remote sensing and 3D city modelling have enabled fine-resolution analysis of microclimates[37,38], their application to shade simulation is constrained. Crucially, few studies differentiate between shaded areas that are publicly accessible and those that are not[19,39], leaving open the question of whether urban shade provisions are a common good or a spatial privilege.

In this study, we present a comparative analysis of pedestrian-accessible shade in nine globally diverse cities: Amsterdam, Barcelona, Belém, Boston, Hong Kong, Milan, Rio de Janeiro, Stockholm, and Sydney. These cities were selected based on multiple criteria: coverage of diverse climatic zones (tropical, temperate, continental, Mediterranean); variation in urban morphology (compact, sprawled, green-integrated); representation across Global North and South contexts; and availability of high-quality, comparable geospatial as well as socioeconomic data. This diversity enables us to identify generalizable patterns and context-specific factors of shade inequality. Using high-resolution shade maps (0.5 × 0.5 m) on the summer solstice day overlaid on pedestrian networks, we quantify the inequality in shade distribution across neighbourhoods and examine its associations with green/grey infrastructure and socioeconomic indicators. Our findings contribute to research at the intersection of climate adaptation and environmental justice.

Results

Uneven shade distribution

To investigate the spatial inequality of urban shade provision under rising heat stress, we analysed the average level of shade in all neighbourhoods of nine globally distributed cities (see Fig. 1a). The average shade metric represents the mean proportion of sidewalk area shaded between 10:00 and 17:00 − the hottest hours of the day − on the respective summer solstice day. Values range from 0 (no shade at any time) to 1 (fully shaded throughout the entire period). In all nine cities, we found substantial intra-urban variation in shade coverage. To compare among global cities, here we define three shade levels: values below 0.4 were categorised as low (insufficient) shade, values between 0.4 and 0.6 as moderate shade, and values above 0.6 as high shade, based on the distribution of average shade across all global neighbourhoods (see data distribution in Supplementary Information).

In Amsterdam, moderate to high levels of shade are primarily concentrated in the central urban areas (average shade over 0.4), while peripheral neighbourhoods show lower shade levels (less than 0.4). In Barcelona, most neighbourhoods exhibit low to moderate shade levels (between 0.4 and 0.6). Only a few scattered districts reach levels above 0.60. This suggests that while shade is somewhat evenly distributed, it remains suboptimal in large parts of the city. Belém presents a starkly different pattern: Low sidewalk shade levels dominate most of the neighbourhoods (less than 0.15), with only small pockets reaching moderate levels. As a tropical city with extensive informal settlements and high heat vulnerability, Belém's overall lack of shaded spaces likely exacerbates exposure to extreme heat, particularly in socio-economically marginalised areas.

Boston exhibits a more moderate distribution. Most neighbourhoods fall between 0.15 and 0.4 in average shade, with some districts in the northern and western parts of the city reaching values above 0.45. Nonetheless, several inner-city areas remain undershaded, revealing spatial inequities in access to cooling infrastructure. In Hong Kong, substantial spatial heterogeneity is evident. Some central and southern neighbourhoods exhibit very high shade levels (above 0.85), while a significant number of areas in northern and peripheral areas remain moderately to poorly shaded (below 0.40). This patchy pattern likely reflects a mix of steep terrain, compact high-rise development, and uneven canopy cover. In Milan, moderate to high shade coverage is widespread. Most neighbourhoods fall between 0.50 to 0.75 in average shade, particularly in central areas with dense, older building stock. However, several outlying districts remain less shaded, likely due to newer, lower-density development patterns.

Rio de Janeiro presents the most extensive coverage of low-shade areas among all cities studied. Vast swaths, particularly in peripheral and hillside neighbourhoods, have an average shade of less than 0.10, often coinciding with informal settlements. Only a few select coastal and affluent districts reach moderate shading levels. Conversely, Stockholm stands out for its consistently high shade provision. Most of its neighbourhoods fall within the 0.6-0.9 range, with some exceeding 0.9. This uniformity likely results from long-term urban planning strategies that integrate tall buildings and narrow street canyons with abundant green infrastructure, which supports pedestrian comfort. In Sydney, a strong spatial divide is observed: Western and southern neighbourhoods exhibit very low shade levels (average shade less than 0.15), while some denser central and northern areas reach moderate shading (0.4- 0.6). These disparities highlight urban heat vulnerability in suburbs with less building density, which often lack tree canopy and street-level shading to compensate for the reduction in building shade.

Together, these analyses reveal a pronounced unevenness in the distribution of urban shade both within and across cities. While cities at higher latitudes, such as Barcelona, Milan, and Stockholm, tend to provide relatively widespread shade, in tropical cities closer to the equator, such as Belém and Rio de Janeiro-where shade is most critically needed due to intense solar radiation-the prevalence of low-shade areas is especially concerning.

Shade injustice in cities

Figure 2 illustrates both the cumulative distribution of key metrics and their spatial representation within selected urban environments in the nine global cities. Per capita income and home value are considered proxies of wealth in this context.

Figure 2a illustrates the cumulative share distributions of shade relative to three socioeconomic variables: total population, income per capita, and home value, using Lorenz curves. The dashed diagonal line in each panel represents perfect equality, where shade would be distributed proportionally to each socioeconomic group. The further the actual curves deviate below this line, the greater the inequality in shade access. The insets in each panel report the Gini coefficients for each city and variable, numerically summarising the degree of inequality. Higher Gini values correspond to greater disparities. Together, the curves and Gini coefficients highlight significant differences in shade equity across cities and socioeconomic groups.

Additionally, a consistent pattern of inequality emerges, with lower-income, lower-home-value, and more densely populated groups receiving disproportionately less shade. Notably, Stockholm exhibits the steepest deviations from the equality line across all dimensions, even though the bottom 20% of neighbourhoods in Stockholm (0.58) still enjoy a higher level of shade than the top 20% of neighbourhoods in Belém (0.37), reflecting high levels of shade inequality despite a generally high baseline of shade provision across the city. In other words, while most of the neighbourhoods in Stockholm are well shaded, wealthier areas benefit from even greater shade coverage, accentuating existing disparities. In contrast, Amsterdam and Boston display curves that are closer to the line of equality for total population, though inequality increases when examined across wealth dimensions. In terms of income, Boston, Hong Kong, Rio de Janeiro,

https://doi.org/10.1038/s41467-026-69190-w

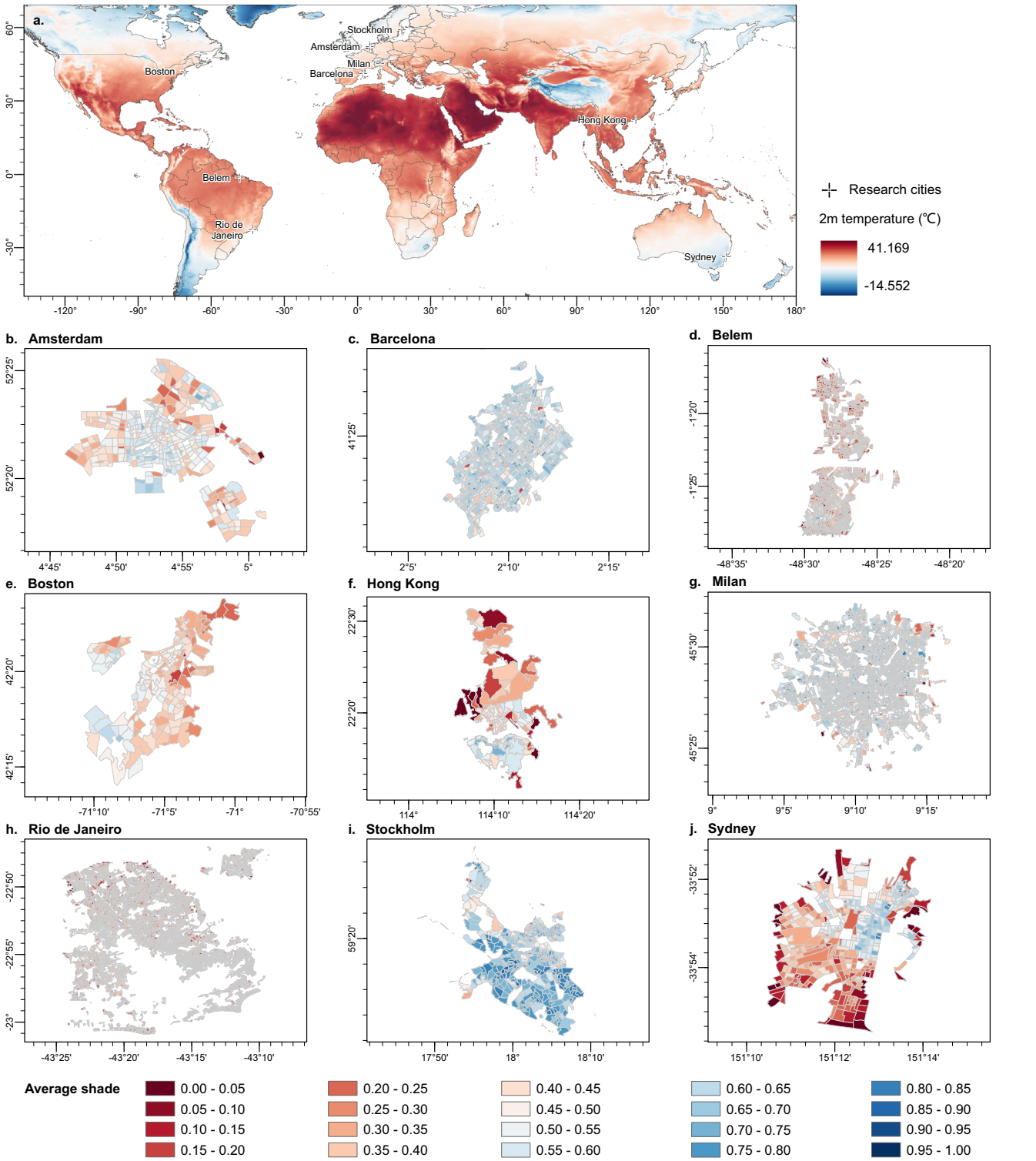

Fig. 1 | Composite maps of global surface temperatures and intra-urban shade disparities. a Global distribution of 2-metre air temperatures averaged over June–August 2024, derived and averaged from the ERA5 Climate Data Store. Warmer regions are denoted by deep red hues, while cooler regions are indicated in blue. The map also highlights nine study cities, marked with black crosses, representing diverse climate zones and urban morphologies. **b**–**j** Spatial patterns of average neighborhood-level shade in nine selected cities: (**b**) Amsterdam ($n = 388$), (**c**) Barcelona ($n = 1014$), (**d**) Belém ($n = 1504$), (**e**) Boston ($n = 169$), (**f**) Hong Kong ($n = 129$), (**g**) Milan ($n = 6428$), (**h**) Rio de Janeiro ($n = 6933$), (**i**) Stockholm ($n = 494$), (**j**) Sydney ($n = 458$).

and Stockholm exhibit high Gini coefficients, followed by Amsterdam, Milan, and Sydney, which present moderate levels of disparity.

At the neighbourhood scale, bivariate spatial mapping further illustrates how average shade is spatially entangled with wealth. Mathematically, the average shade is divided into three quantile-based categories (tertiles), labelled from low to high. Each urban unit reflects the combination of its Per Capita Income level (Low, Medium, High) and its Average Shade level (Low, Medium, High).

In Amsterdam, areas predominantly in the medium-to-high per capita income range are combined with medium-to-high average

https://doi.org/10.1038/s41467-026-69190-w

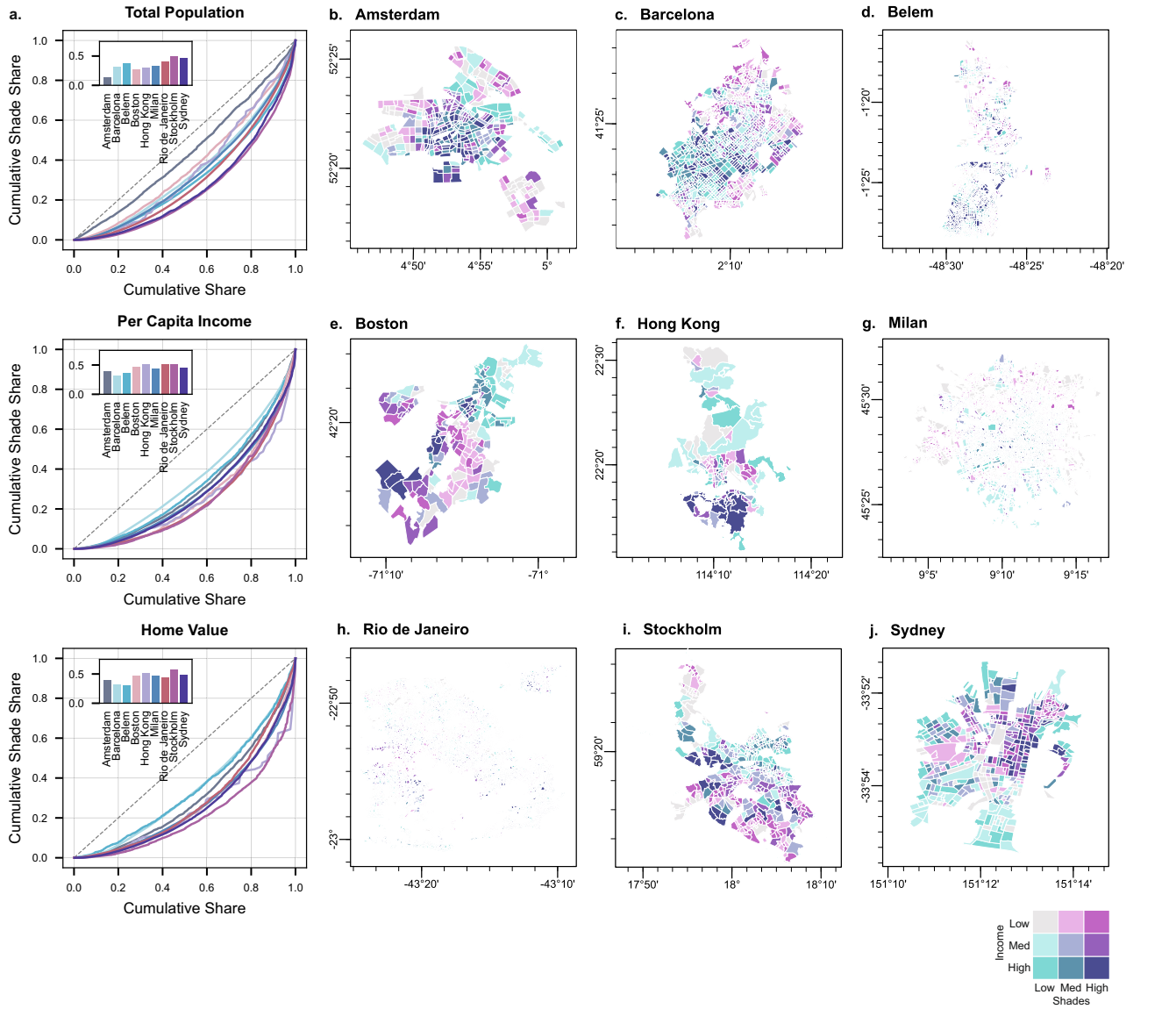

Fig. 2 | Neighbourhood-level shade inequalities in cities. a Gini coefficients and Lorentz curves for each city. **b**–**j** Bivariate map of average shade and per capita income at neighbourhood scale in nine selected cities: (**b**) Amsterdam, (**c**) Barcelona, (**d**) Belém, (**e**) Boston, (**f**) Hong Kong, (**g**) Milan, (**h**) Rio de Janeiro, (**i**) Stockholm, (**j**) Sydney.

shades, suggesting a positive spatial correlation between these two characteristics. There are fewer areas indicating low income or low average shades. In Barcelona, many neighbourhoods fall into the low-to-medium income and low-to-medium shade categories, forming clusters of pink and lavender tones. However, the distribution is less spatially polarised compared to cities like Belém or Rio de Janeiro, suggesting more integrated patterns despite existing disparities. Belém demonstrates pronounced spatial segregation. Clearly, large and contiguous areas are dominated by low per capita income combined with low average shades, juxtaposed with areas showing higher per capita income and higher average shades. This pattern suggests significant spatial disparities and a strong positive correlation between low income and low shades, and high income and high shades.

Boston presents a mosaic-like complex pattern that indicates varied pockets of socio-economic characteristics. For instance, there is a significant mix of different level combinations (e.g., medium income with varying shades, or low income with medium/high shades). In Hong Kong, extreme spatial segregation is visible, with distinct clusters of low-income/low-shade areas (light pink) and high-income/high-shade zones (deep blue). The northern urban areas stand out for their concentration of underserved neighbourhoods, whereas southern and central zones benefit from both higher income and greater shade provision. Milan's urban fabric reveals relatively mixed combinations, though wealthier central areas tend to align with better shading. A ring of lower-income and lower-shade areas surrounds the core, indicating moderate spatial stratification.

Similar to Belém, Rio de Janeiro exhibits a highly heterogeneous and often starkly contrasting spatial bivariate distribution. Areas dominated by low per capita income and low average shades frequently appear in close proximity to areas with higher per capita income and higher average shades. This pronounced spatial variability highlights significant within-city income inequality and segregation, often in strong correlation with the average shade. Stockholm exhibits a more dispersed but still distinct spatial structure, resembling that of Amsterdam. While some regions show higher per capita income combined with higher average shades, other areas suggest medium per capita income or a combination with lower average shades. Sydney displays a prominent pattern of high-income neighbourhoods (especially in the northeast and coastal areas), coinciding with higher

https://doi.org/10.1038/s41467-026-69190-w

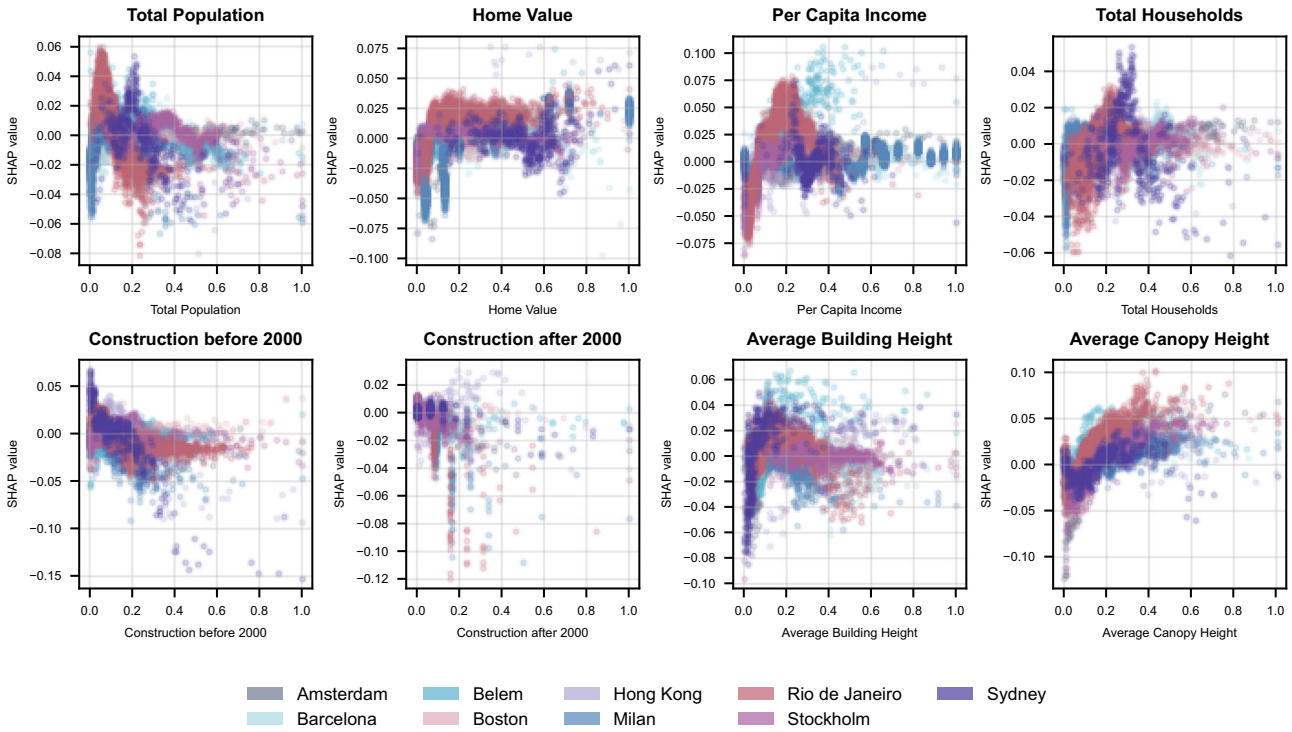

Fig. 3 | Regression results of the interpreted XGBoost model with SHAP interpretation for nine cities. Notes: Each plot shows the relationship between the standardised feature values (X-axis) and the corresponding SHAP values (Y-axis), which indicate the contribution of each feature to the prediction of average shades.

average shade. In contrast, large expanses of western suburbs show clusters of low income and low shading. This highlights a clear east-west divide in environmental equity.

Associations of shade and income

We investigated the relationship between various socioeconomic and urban form indicators and the average shades metric across a diverse set of global cities. Our analysis, presented in Fig. 3, utilised a tree-based ensemble learning approach (XGBoost) and SHAP (SHapley Additive exPlanations) to elucidate these relationships. Detailed information and model performance of each city can be found in the Supplementary Information.

Across all cities (see Fig. 3), average canopy height emerged as the most influential and positively correlated predictor of urban shade provision. SHAP dependence plots indicate a near-monotonic increase in SHAP value with increasing canopy height, particularly pronounced in Amsterdam, Belém, Boston, Rio de Janeiro, and Stockholm. This underscores the fundamental role of mature urban vegetation in mitigating heat stress via shade. Likewise, average building height exhibited a consistent positive association with shade, particularly in compact cities with dense vertical development (e.g., Boston and Hong Kong), where taller structures provide shading to adjacent sidewalks.

The effect of socioeconomic indicators-per capita income, home value, and total population-on shade provision was more heterogeneous. In several cities, including Amsterdam, Belém, Boston, Hong Kong, and Stockholm, lower per capita income and home values were associated with systematically lower SHAP values, suggesting under-investment in shade infrastructure in lower-income areas. This is consistent with observed spatial inequities and Gini-based analyses (see Fig. 2). Conversely, cities like Barcelona and Milan displayed that lower per capita income was more associated with higher average shade. For Rio de Janeiro and Sydney, the medium- and high-income populations have more potential to experience larger shade provisions.

In multiple cities, total population and average shade show a negative correlation, while total households show a neutral correlation, or even a slight positive correlation. In Belém, Hong Kong, Milan, and Rio de Janeiro, increasing population and decreasing households correlated with reduced shading, possibly reflecting overcrowding in low-infrastructure neighbourhoods. Particularly for cities Belém and Rio de Janeiro in Brazil, neighbourhoods with larger populations are often accompanied by a reduction in the emergence of high-density, low-infrastructure urban forms, thereby substantially reducing shade provision. By contrast, an increase in the number of households does not necessarily imply overcrowding. Instead, it may reflect the proliferation of small- and medium-sized housing units, which may have a larger home value.

Disparate building and additional tree shade

Our main analysis is on combined shade on the summer solstice, because this metric captures the aggregate shading environment that residents experience when solar geometry produces the annual minimum horizontal shadowing, and because it provides a single, comparable summary of the competing contributions of buildings and trees. Outside of this comparison, we recommend that potential individual shade targets and policies be based on the hottest month of the year.

Therefore, to further validate and discuss the spatial patterns of the combined shade on the summer solstice, the study generated the combined shade, including building shade and additional tree shade, all on the summer solstice day and the hottest day during the period from 1991 to 2020. Figures 4–7 demonstrate the comparison between these six shade types in Rio de Janeiro and Stockholm; the other cities are presented in the Supplementary Information. These two cities, presented here, as they demonstrate the greatest inequality in urban shade across income groups, also represent the typical cities of the Global North and Global South.

Lorenz curves and Gini coefficients show that building shade is the most evenly distributed of the three metrics, while combined

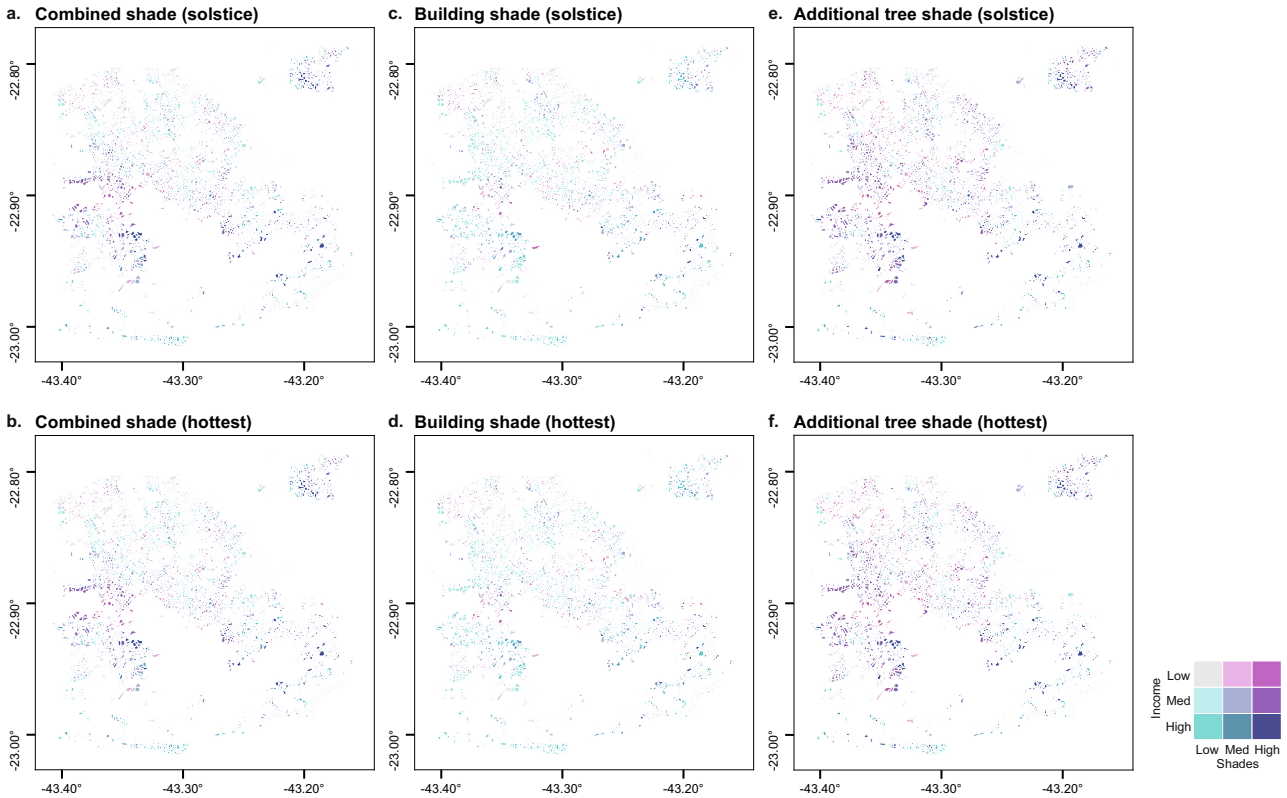

Fig. 4 | Neighbourhood-level shade inequalities in Rio de Janeiro. Spatial pattern of the (**a**) combined shade on the summer solstice day, (**b**) combined shade on the hottest day, (**c**) building shade on the summer solstice day, (**d**) building shade on the hottest day, (**e**) additional tree shade on the summer solstice day and (**f**) additional tree shade on the hottest day. Notes: The additional tree shade represents the additional contribution of trees to urban shade, subtracting from the combined and building shade.

shade and additional tree shade are progressively more unequal, a ranking that is conserved across population, income and housing-value stratifications. Crucially, the separated analyses that we can and do perform are consistent with the combined-shade findings: trees and their shade coverage, are indeed more strongly concentrated in wealthier neighbourhoods, and buildings produce concentrated shade in high-density cores, but these differentiated patterns do not alter the overall conclusion that shade cover is spatially unequal.

Meanwhile, when we directly compare the summer solstice with the single hottest day of the year, the bivariate maps overlapping shading coverage and per capita income at neighbourhood-level change only minimally: all shade types show only modest, localised intensity or boundary adjustments rather than systematic reallocation of shade across neighbourhoods. These results indicate that the macroscopic pattern of shade inequality across the nine cities is robust to day-to-day variations in solar angle in our aggregation framework and is primarily driven by the underlying spatial distributions of built form and canopy rather than by transient solar geometry.

Discussion

Urban shade serves as a critical microclimatic amenity, mitigating thermal stress and enhancing outdoor habitability, particularly during hot seasons[40–42]. Our findings directly engage the unresolved question raised earlier in the paper: whether urban shade provisions constitute a common good or a spatial privilege. The evidence strongly suggests that, in practice, shade often operates as the latter[14,28]. It is important to note, however, that not all shade is intentionally provided as an amenity. Unlike trees or dedicated shade structures, buildings are not constructed with the explicit purpose of shade provision but for residential, commercial, or infrastructural purposes. Their form, density, and spatial configuration generate consequential shading patterns as a by-product of development.

Our analysis reveals a persistent and striking disparity in the average shade available to different urban populations at the neighbourhood level, with larger and denser urban centres often exhibiting higher levels of average shade for wealthier populations. While total population shows a negative association with average shade across cities—suggesting that growing urban populations are not matched by proportional increases in shade provided by grey and green infrastructures—we also uncover that higher home values and per capita incomes, as well as low-density neighbourhoods, are often positively associated with shade. These patterns reveal that shade is not distributed according to universal need or public entitlement (as would be expected of a common good), but rather reflects historical and ongoing disparities in urban investment, land use policy, and political voice. In this light, shade emerges less as a collectively provided amenity and more as a marker of spatial privilege, reinforcing broader structures of environmental injustice.

This finding points to a deeper structural issue of shade inequality, where access to urban cooling resources is not only limited in absolute terms, but also distributed inequitably across socio-demographic lines[43,44]. In particular, Fig. 2 highlights that intra-urban shade distribution is far from uniform, with peripheral and lower-income neighbourhoods often experiencing significant shade deficits. These disparities are not random; rather, they reflect the long-standing legacy of urban planning decisions, land use patterns, and greening policies that have historically favoured certain districts and people over others.

Importantly, inequality does not always stem from scarcity. For example, Stockholm exhibits some of the highest average shade

https://doi.org/10.1038/s41467-026-69190-w

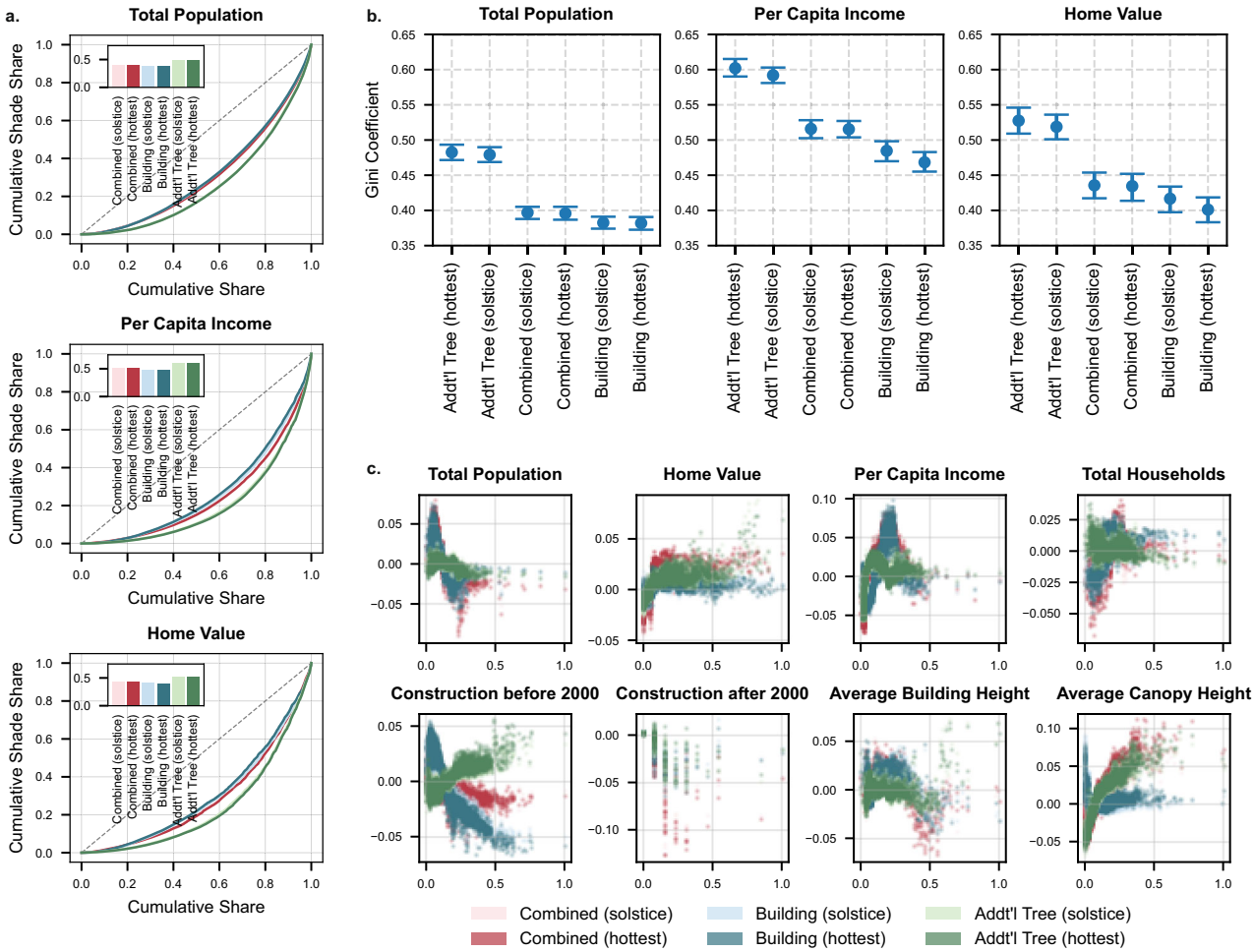

Fig. 5 | Gini coefficient and interpreted the XGBoost model in Rio de Janeiro. **a** Gini coefficients and Lorentz curves for each shade type, (**b**) Confidence Intervals for the Gini coefficient for each shade type (n=6,933, data are presented as mean values +/− SEM), and (**c**) Regression results of the interpreted XGBoost model with SHAP interpretation for each shade type.

coverage among all cities studied, yet also has one of the highest levels of inequality. This pattern of differential abundance—where most areas are adequately shaded, but affluent neighbourhoods benefit from even greater provision—underscores how environmental privilege can persist even in cities that perform well on average. It is not only the absence of shade that matters, but who has more, and how much more, in relation to others.

Our findings build on and extend the work of Chakraborty et al.[16], who showed that urban heat disproportionately affects lower-income groups, largely due to uneven urban vegetation density. While their study focused on the moderating effect of green space on surface temperatures, our analysis pivots toward shade coverage in public pedestrian space—a metric with immediate relevance to human thermal comfort and daily exposure. This distinction matters: broad vegetation coverage, particularly on private land, does not guarantee equitable or accessible cooling benefits.

As Turner et al. argue, shade is one of the most effective and intuitive strategies to reduce heat stress—capable of lowering perceived thermal load by up to 20-40°C[14]. Yet, most cities lack systematic policies to monitor, plan, or equitably distribute shade. In line with their call to assess heat burden based on human experience, our approach quantifies shade at the scale of public pedestrian infrastructure, highlighting who benefits from shade, when, and where. By focusing on publicly accessible, walkable areas—rather than green coverage alone—we expose a key dimension of heat inequity that remains overlooked in conventional planning.

We further find that uneven shade distribution is often amplified in cities with intensive vertical development. As shown in Fig. 3 and Supplementary Information, high-rise urban cores—despite having limited tree cover or pedestrian-friendly infrastructure—can create significant ground-level shading. These dense, vertical environments sometimes act as cool oases under a warming climate[45,46]. Conversely, suburban neighbourhoods with fewer tall buildings show much lower average shade, exacerbating human heat exposure.

Our regression analysis underscores the importance of evaluating environmental resources such as shade through the lens of human exposure. Traditional landscape-level assessments may overstate the real-world benefits of urban greening by ignoring who has access to shaded pedestrian areas. Once population and wealth distribution are considered, effective access to shade reveals stark inequalities. This calls for a shift from areal averages to people-centred shade equity frameworks[14,41].

The policy implications are profound. As climate extremes intensify, ensuring equitable access to shade must become a central goal of urban resilience planning. This includes targeted investments in tree planting, green corridors, and shading infrastructure—particularly in disadvantaged neighbourhoods. Simply increasing overall green coverage is insufficient if spatial inequalities persist[47,48].

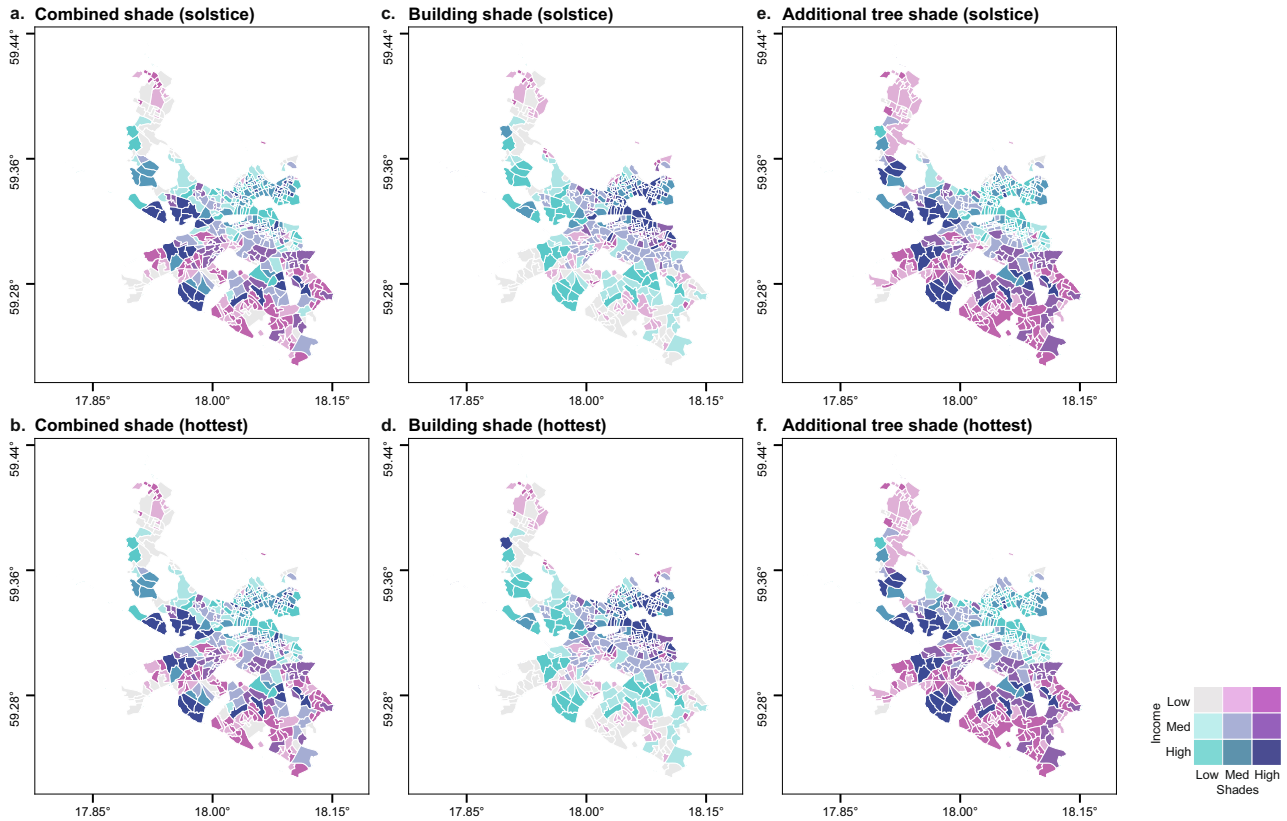

Fig. 6 | Neighbourhood-level shade inequalities in Stockholm. a Combined shade on the summer solstice day, (**b**) combined shade on the hottest day, (**c**) building shade on the summer solstice day, (**d**) building shade on the hottest day, (**e**) additional tree shade on the summer solstice day, and (**f**) additional tree shade on the hottest day.

Finally, our findings highlight the urgent need to address uneven shade distribution not only as a climate adaptation issue but as a matter of environmental justice and public health. The juxtaposition of high population density and low shading in many global cities exposes millions to amplified heat risks, while affluent neighbourhoods continue to enjoy cooling benefits. Bridging this gap will require coordinated urban design, policy reform, and community-led action to ensure that shade—like any critical urban resource—is accessible to all.

We also acknowledge several limitations that point toward directions for future research. First, our shade simulation focuses on shades cast by buildings and trees, which are the primary contributors to heat mitigation at the urban scale[41]. Other forms of artificial shading (e.g., pergolas, shade sails) may offer localised benefits, but were not included here due to data limitations and inconsistent availability across cities[39]. Moreover, it is essential to recognise that the cooling benefits of shade vary significantly between buildings and trees. As trees not only provide physical shade but also deliver additional cooling through evapotranspiration[18,20], thereby benefiting adjacent public spaces even when direct access to green areas is limited, while built structures may have more constrained effects. Future assessments could therefore distinguish between these sources of shade to better capture their heterogeneous contributions to urban microclimates and human thermal comfort.

Second, socio-demographic indicators vary by country, and although we screened and selected the most reliable available datasets, these are not perfectly comparable with each other. Future work should integrate more diverse data sources-particularly for cities in the Global South, where census data are often lacking at the neighbourhood scale-to assess shade inequalities better and identify vulnerable hotspots in need of targeted interventions.

Third, due to the lack of harmonised sidewalk datasets across cities, we used a generative approach based on OpenStreetMap street networks to estimate pedestrian space. While this enabled consistent cross-city comparisons, it introduces uncertainty in the exact location and extent of walkable areas. In cities with extensive sidewalks but relatively low pedestrian activity (e.g., Boston)[49,50], our simulations may overestimate the effective shade experienced by people, suggesting that future work could incorporate measures of walkability or pedestrian usage. Conversely, in cities where sidewalks are scarce or fragmented (e.g., Belém and Rio de Janeiro)[51], our estimates likely underestimate available shade, highlighting the need for improved sidewalk mapping and inclusion of informal pedestrian paths. Accurate, high-resolution sidewalk data is essential for targeting shade interventions to the areas where people actually move and dwell.

Methods

Shade map simulation

To evaluate shade availability across urban neighbourhoods, we generated high-resolution shade maps for nine globally distributed cities: Amsterdam, Barcelona Belém, Boston, Hong Kong, Milan, Rio de Janeiro, and Sydney. As shown in Fig. 1, these cities span a broad range of climatic zones − from temperate (e.g., Amsterdam, Stockholm) to tropical and subtropical regions (e.g., Belém, Hong Kong, Sydney) − providing a comparative basis for analysing shade provision under differing environmental and urban morphological conditions.

The shade maps (0.5 m × 0.5 m resolution) were produced using a standardised pipeline adapted from the Slim Shady study[41] and extended in Sun Blocked[52]. The methodology combines a Digital Surface Model (DSM) as well as a tree detection and segmentation workflow from aerial imagery to model shadows cast by buildings and trees at scale. Shadow simulations were conducted using a standalone implementation of the UMEP Shadow Generator[53], which computes solar obstruction based on sun position, object height, and geometry.

https://doi.org/10.1038/s41467-026-69190-w

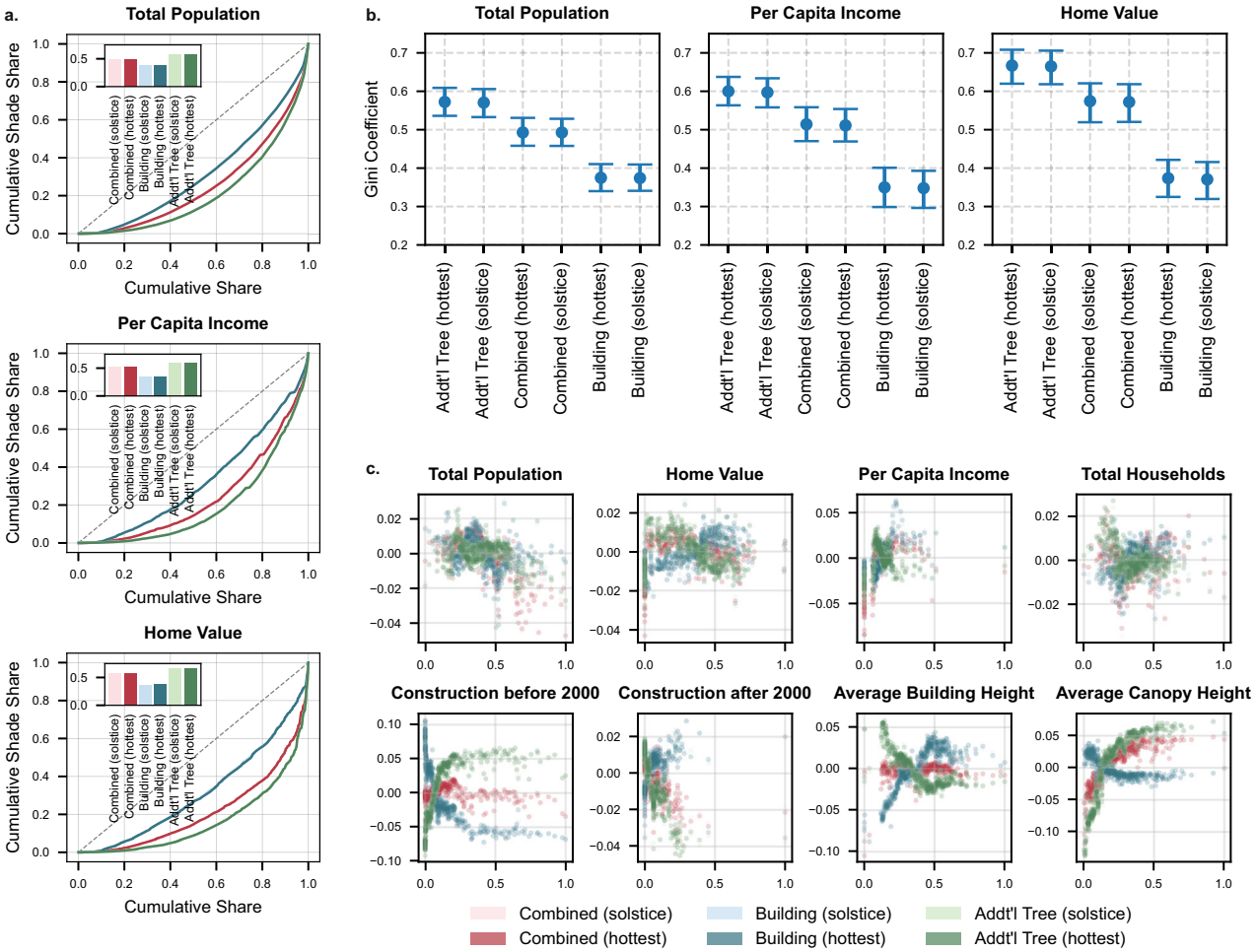

Fig. 7 | Gini coefficient and interpreted the XGBoost model in Stockholm. a Gini coefficients and Lorentz curves for each shade type, (**b**) Confidence Intervals for the Gini coefficient for each shade type ($n = 494$, data are presented as mean values +/− SEM), and (**c**) Regression results of the interpreted XGBoost model with SHAP interpretation for each shade type.

All cities except Amsterdam used DSM data from the Google Solar API (HIGH tier), derived from low-altitude aerial imagery processed photogrammetrically at 0.1 m spatial resolution, with elevations referenced to the EGM96 geoid. In Amsterdam, Solar API coverage was incomplete, likely due to the presence of the national LiDAR dataset. We therefore substituted the Actueel Hoogtebestand Nederland (AHN4) as the DSM source. AHN4 is a nationwide airborne LiDAR dataset acquired between 2019 and 2022 with a nominal point density of 6–10 points per m^2 and a reported vertical accuracy of approximately 5 cm ($RMSE_z$) under flat, open conditions[54]. This substitution ensured complete coverage and maintained high geometric accuracy for shade simulation in Amsterdam.

To account for partial solar penetration through vegetation, we applied a transmissivity value of 10%, allowing 10% of direct solar radiation to pass through tree crowns. This setting is consistent with prior work on the radiative impact of urban trees on pedestrian exposure[55]. Therefore, a value of 0 to 1 is given to the shade map, where 0 indicates the pixel is fully shaded during the time frame, and 1 is fully sunlit.

Half-hourly shade conditions were simulated for a representative summer solstice day (June 21 in the Northern Hemisphere, December 21 in the Southern Hemisphere) and additionally the equinox for Belém (March 21), where the solar angle is at its minimum. The summer solstice was chosen as the primary reference day because it represents the maximum potential solar exposure for a given location, providing a consistent and comparable baseline across cities for understanding shading distribution under ideal conditions. The simulated result is a stack of half-hourly binary shade rasters per city, which were then aggregated to calculate the shade metrics (shown in the next Section) per sidewalk polygon or pixel, representing the proportion of time that location is shaded during peak daytime hours. The temporal pattern for each city can be found in the Supplementary Information.

To delineate pedestrian space consistently across all cities, we used KerbSide[56], an open-source custom pipeline built on osm2streets, to generate standardised sidewalk and footpath polygons from OpenStreetMap street network data. This approach was chosen to reflect the absence of harmonised, high-resolution pedestrian infrastructure data across most cities, while introducing a controlled and transparent source of structural error. Although it cannot capture all local nuances (e.g., exact sidewalk widths, positions, or informal paths), it ensures a consistent basis for inter-city comparison.

This approach captures both the spatial extent and temporal persistence of shade, enabling robust comparison of shade coverage across different urban contexts. Similar to prior work, we focus specifically on publicly accessible walkable areas where shade is most critical for outdoor thermal comfort and mobility.

To ensure analytical consistency and avoid bias from fringe or sparsely populated zones, we excluded neighbourhoods from analysis if they met one of two criteria: 1) Insufficient data for shade simulation, such as missing DSM or vegetation layers, and 2) Neighbourhoods with extremely low population density, defined as falling below the 5th percentile of the city-specific population density distribution. These

Table 1 | Descriptions of socioeconomic indicators

Indicator	Description
Total Population	Represents the number of residents in each neighborhood. In inequality analysis, it is used to determine if larger populations receive disproportionately less or more shade.
Total Households	Serves as an alternative to population. It can help control for household clustering effects in shade access.
Per Capita Income	Reflects average income levels and is a direct measure of socioeconomic status. Its inequality indicates whether wealthier areas receive better shading, suggesting environmental privilege.
Home Value	Acts as a spatially sensitive proxy for neighbourhood affluence and long-term investment. Higher home values may correlate with greener streetscapes or more shaded infrastructure due to private or municipal investment.

typically correspond to non-residential areas such as airports, industrial areas, and natural reserves in cities.

For further validation, the study applied this same workflow to generate the combined shade, building shade, and additional tree shade, all on the summer solstice day and the historical hottest day. The hottest day for each city was identified as the maximum temperature (tmax) over 30 years, using the 1991-2020 climate normals from local weather stations.

Urban shade metrics

To assess shading conditions within urban neighbourhoods, we developed two complementary metrics derived from spatial zonal statistics: Average shade intensity and cumulative shade resource. These indicators jointly capture the intensity and total availability of shade, making them respectively suitable for correlation analyses with socio-economic variables and for evaluating spatial inequities in shade distribution. Critically, both metrics were computed consistently across all study cities using the following two-step procedure:

(1) The high-resolution shade raster map was first masked using sidewalk polygons to restrict analysis to pedestrian-accessible surfaces;
(2) Zonal statistics were then applied to aggregate sidewalk-level shade values to the neighbourhood level, yielding a single average shade intensity per neighbourhood.

These steps confirm that our shade metrics are derived exclusively from publicly accessible pedestrian spaces: non-public areas (e.g., building footprints, private lots) were excluded during the sidewalk masking step, ensuring that all reported shade averages reflect conditions experienced by pedestrians. In the Supplementary Information, we provide summary statistics on the distribution of sidewalk areas and neighbourhood sizes across all study cities, as well as potential estimation bias due to neighbourhood size variability.

Therefore, the average shade intensity (proportion from 0 to 1) provides a normalised, dimensionless measure of average shade across all sidewalk pixels within the neighbourhood i:

$$\text{average shade}_i = 1 - \text{average sunlit}_i \quad (1)$$

where: average shade$_i$ denotes the average shade coverage across all sidewalk pixels within the neighbourhood i (0 = never shaded, 1 = always shaded), and average sunlit$_i$ is the corresponding normalised sunlit intensity. All polygon areas were calculated in appropriate projected coordinate systems to ensure metric accuracy. The entire workflow-including coordinate reference system alignment, raster-vector integration, and metric computation-was implemented using Python libraries (pandas, geopandas, and rasterstats).

Due to its normalised, unitless form, average shade intensity is appropriate for correlation and regression analyses with socio-economic indicators (e.g., income, home value indicators). It enables meaningful comparisons across areas of different sizes and reduces bias from unequal spatial extent.

Meanwhile, the cumulative shade resource (in m^2) quantifies the total shaded area available to pedestrians within a neighbourhood. It is calculated by multiplying the average shade$_i$, and the sidewalk area$_i$:

$$\text{cumulative shade}_i = \text{average shade}_i \times \text{sidewalk area}_i \quad (2)$$

where: sidewalk area$_i$ is the total area of sidewalk (in m^2) within the neighbourhood i, after masking out non-pedestrian surfaces such as buildings and private lots.

Because the cumulative shade resource reflects the absolute quantity of shading, it allows for assessing distributional inequities across urban space. When aggregated across socio-demographic groups, it can be used as input for calculating the Gini coefficient or other inequality indices. This helps reveal whether shade is equitably distributed relative to population or vulnerability metrics. For validation, the temporal patterns of average shade from sunrise to sunset can be found in the Supplementary Information, all showing the U pattern during the whole period.

In this study, we focus on the performance of these two indicators during the period when people are outdoors for leisure activities, 10:00 and 17:00. As well as the sunshine will be more intense during this period because of the intense solar radiation[57], shade is needed more as a cooling facility[58]. Once the average shade intensity and cumulative shade resource were calculated for each half hour, we averaged them to characterise the average performance for this period.

Socioeconomic indicators

Considering the census data accessibility at the neighbourhood level for research cities, we selected four key socioeconomic variables to assess the social distribution and equity of urban shading[13,59]. All these socioeconomic indicators were retrieved from local government websites from 2019 to 2023. The data availability statement details the data source for each city.

As shown in Table 1, these variables capture population scale, economic well-being, and income stratification, and serve as the basis for two complementary analytical frameworks: regression modelling using average shade intensity and inequality assessment using cumulative shade resource. Notably, the socioeconomic data are not uniformly expressed or formatted across different cities. However, since neighbourhood inequality is analysed separately within each city, these inter-city differences do not affect the validity of the disparity comparison.

Notedly, even though home values do not adequately represent the economic realities of individuals, amounts of previous studies have proven that home value can indirectly reflect overall housing costs-including the rental market-and community wealth levels as an outcome of shared drivers such as location, public investment, and environmental quality[60–62]. Therefore, home value serves as a proxy for area-level affluence and long-term investment, alongside per capita income as complementary indicators of neighbourhood socio-economic status.

Gini coefficient

To assess whether cumulative access to shade is equitably distributed across different population and income groups, we calculated population-weighted Gini coefficients for each city based on neighbourhood-level data. The Gini coefficient is widely used to quantify inequality in resource distribution[29,59]. A Gini value of 0 indicates a perfectly equal distribution of shade across residents, whereas values approaching 1 reflect high inequality, where most shade is concentrated in a small share of the population or wealth.

In this study, it is adapted to evaluate disparities in cumulative shading exposure, a critical environmental resource in the context of urban heat and climate adaptation. We considered three socioeconomic indicators: total population, per capita income, and average home value. These indicators represent both demographic size and economic status, which may influence access to shading and reflect underlying urban form and planning priorities. To ensure that neighbourhoods with more residents contribute proportionally to the inequality measure, we calculated a population-weighted Gini coefficient for each city.

Specifically, neighbourhoods ($j = 1, \ldots, n$) were ranked in ascending order of total shading exposure (y_j)., and the cumulative population-weighted shares of shade Y_i and socioeconomic indicator X_i were calculated as:

$$X_i = \frac{\sum_{j=1}^{i} w_j}{\sum_{j=1}^{n} w_j},\ Y_i = \frac{\sum_{j=1}^{i} w_j y_j}{\sum_{j=1}^{n} w_j y_j} \tag{3}$$

where w_j represents the weighting factor for the neighbourhood j, and y_j denotes the total shade exposure in the same neighbourhood.

The Gini coefficient (G) was then obtained using the trapezoidal rule for numerical integration along the Lorenz curve:

$$G = 1 - \sum_{i=1}^{n-1} (X_{i+1} - X_i)(Y_{i+1} + Y_i) \tag{4}$$

To assess the robustness of the Gini estimates and account for sampling variability across neighbourhoods, we additionally calculated 95% confidence intervals using a non-parametric bootstrap procedure. The resulting confidence intervals are reported in the Supplementary Information.

Regression analysis

We further utilised an interpretable machine learning regression model to investigate the relationship between average shade intensity and a range of socioeconomic and urban form variables. The aim was to identify patterns of association across neighbourhoods, especially those that might signal inequities in shade provision or planning priorities.

The predictors we included spanned population and household counts, income and home value levels, construction era (before and after 2000), and two physical descriptors of the built environment, including building height and average tree canopy height[63,64]. These variables were chosen to reflect the multidimensional nature of urban neighbourhoods-capturing both social conditions and morphological features-without assuming any direct causal pathway to shade availability.

Regarding the average canopy height, we obtained the canopy height map at a 1 m spatial resolution[64]) and averaged it at the neighbourhood level. For the building-related variables, the study utilised the long-term global land cover remote sensing data at 30 m spatial resolution[65]) and overlapped it with building polygons data containing building heights attributes[63,66]) to filter out buildings built before or after 2000. Besides, these building polygons can be used to calculate the average height of all buildings for each neighbourhood.

Although the construction years of the buildings are mutually exclusive, we separated them into two variables, considering that their effects are not completely mirror images of each other. Pre-2000 buildings often reflect historical planning practices, which may be associated with narrow, shaded streets in some cities, or lower-density development in others. Conversely, post-2000 construction typically adheres to more modern building codes, often featuring high-rise buildings and different urban design principles. They will show different relationships with average shade. Besides, this also considers that a district with a high proportion of pre-2000 buildings might have a small total building count, while another with a similar proportion might have a very large one.

To understand the relationships between each variable and average shade, we trained an XGBoost regression model to capture the complex, nonlinear effects among the predictors[67,68]. Data from multiple cities with varying sample sizes were pooled, and sample weights proportional to city-specific sample sizes were applied during model training to mitigate biases due to uneven data distributions.

We modelled the relationship between shade intensity ($\hat{y}$) and a set of predictors $X = \{x_1, x_2, \ldots, x_p\}$ using an XGBoost regression function $f(\cdot)$ trained via gradient boosting:

$$\hat{y} = f(X) = \sum_{m=1}^{M} f_m(X),\ f_m \in \mathcal{F} \tag{5}$$

where $\mathcal{F}$ denotes the space of regression trees. Model hyperparameters-including the number of trees, tree depth, learning rate, subsample ratio, and column sampling ratio-were optimised using cross-validated grid search to minimise the prediction error across five folds:

$$\mathcal{L}(y, \hat{y}) = \frac{1}{n} \sum_{i=1}^{n} (y_i - \hat{y}_i)^2 + \sum_{m=1}^{M} \Omega(f_m) \tag{6}$$

This approach provided a flexible and high-performing method for identifying associations across diverse urban contexts, while accounting for differences in sample sizes among cities. Model performance was evaluated using R^2, RMSE, and MAE, and feature importance was quantified not only by SHAP values but also by XGBoost-specific metrics, including Weight, Gain, and Cover, which reflect the frequency, contribution, and coverage of each predictor across all regression trees (see Supplementary Information).

To interpret the model outputs, we employed SHAP (SHapley Additive exPlanations) values to evaluate the marginal contribution of each feature to the predicted average shade[58,69], where the contribution of a feature x_j to the prediction for an observation i is represented by $\phi_j^{(i)}$, such that

$$f(x^{(i)}) = \phi_0 + \sum_{j=1}^{p} \phi_j^{(i)} \tag{7}$$

The SHAP framework enabled both global variable importance ranking and visualisation of the dependence between each predictor and its impact on model output, accounting for nonlinearity and feature interactions. This allowed us to examine how predicted shade levels vary with changes in specific features and to identify potential inequalities embedded in urban form and socioeconomic structure.

Reporting summary

Further information on research design is available in the Nature Portfolio Reporting Summary linked to this article.

Data availability

The high resolution of the Digital Surface Model (DSM) was retrieved from Google Solar API. The global building polygon dataset for each

city was retrieved from UT-GLOBUS for city-scale urban simulations and 3D-GloBFP: global three-dimensional building footprint dataset. The canopy height map at 1m spatial resolution was retrieved from Canopy height maps from RGB imagery. The land cover data before 2000 was retrieved from Global Land Cover and Land Use Change, 2000-2020. Socioeconomic indicators for each city at the neighbourhood level were retrieved from their corresponding official open data: 1) Yearly key figures for neighbourhoods in Amsterdam were retrieved from the CBS databank. 2) Census statistics (2021) in Barcelona: Open Data Barcelona and Idescat. Open Data. 3) Census data and geographical boundaries of Belém and Rio de Janeiro were retrieved from the IBGE and Censo 2022 | IBGE. 4) American Community Survey 5-Year Data (2019-2023) were retrieved from the U.S. Census Bureau by API. 5) Statistics and Boundaries of Small Tertiary Planning Unit Groups (2021) in Hong Kong were retrieved from the Common Spatial Data Infrastructure (CSDI) Portal. 6) Census data and geographical boundaries of Milan (2021) were retrieved from the Comune di Milano, Istat, Dipartimento delle Finanze and Maurizio Napolitano. 7) Demographic Statistical Data and Areas of Stockholm (2025) were retrieved from the Open data for DeSO and the Dataportalen. 8) 2021 Census statistics and geographical boundaries of Sydney were retrieved from the Australian Bureau of Statistics. The data generated and used in this study have been deposited in Zenodo: https://doi.org/10.5281/zenodo.17972371.

Code availability

The codes and libraries used in the analysis can be accessed here: https://doi.org/10.5281/zenodo.17972371.

References

1. Yuan, Y. et al. Surface urban heat island effects intensify more rapidly in lower income countries. *npj Urban Sustain.* **5**, 1–11 (2025).
2. Huang, W. T. K. et al. Economic valuation of temperature-related mortality attributed to urban heat islands in European cities. *Nat. Commun.* **14**, 7438 (2023).
3. Rocha, A. D. et al. Unprivileged groups are less served by green cooling services in major European urban areas. *Nat. Cities* **1**, 424–435 (2024).
4. Klingelhöfer, D., Braun, M., Brüggmann, D. & Groneberg, D. A. Heatwaves: does global research reflect the growing threat in the light of climate change? *Globalization Health* **19**, 56 (2023).
5. Sias, J. E. et al. Climate change impacts on roadways. *Nat. Rev. Earth Environ.* **6**, 555–573 (2025).
6. Janatabadi, F., Ortiz, L. & Ermagun, A. Extreme heat threatens railroads with connectivity and ridership loss in the United States. *npj Urban Sustain.* **5**, 37 (2025).
7. Wang, S. et al. Dual impact of global urban overheating on mortality. *Nat. Clim. Change* **15**, 497–504 (2025).
8. He, C. et al. The inequality labor loss risk from future urban warming and adaptation strategies. *Nat. Commun.* **13**, 3847 (2022).
9. Masuda, Y. J. et al. Warming from tropical deforestation reduces worker productivity in rural communities. *Nat. Commun.* **12**, 1601 (2021).
10. Perera, A. T. D. et al. Challenges resulting from urban density and climate change for the EU energy transition. *Nat. Energy* **8**, 397–412 (2023).
11. Haddad, S. et al. Quantifying the energy impact of heat mitigation technologies at the urban scale. *Nat. Cities* **1**, 62–72 (2024).
12. Marcińczak, S., Iglesias-Pascual, R., Kopeć, D., Wróbel, K. & Mooses, V. Landscapes of thermal inequality: Exploring patterns of climate justice across multiple spatial scales in Spain. *Landsc. Urban Plan.* **254**, 105255 (2025).
13. Shreevastava, A. et al. Contemporary income inequality outweighs historic redlining in shaping intra-urban heat disparities in Los Angeles. *Nat. Commun.* **16**, 4950 (2025).
14. Turner, V. K., Middel, A. & Vanos, J. K. Shade is an essential solution for hotter cities. *Nature* **619**, 694–697 (2023).
15. Martinez, S. et al. A methodology to bridge urban shade guidelines with climate metrics. *Sustain. Cities Soc.* **124**, 106322 (2025).
16. Chakraborty, T., Hsu, A., Manya, D. & Sheriff, G. Disproportionately higher exposure to urban heat in lower-income neighborhoods: a multi-city perspective. *Environ. Res. Lett.* **14**, 105003 (2019).
17. Endreny, T. A., Ciolfi, M., Endreny, A., Chiocchini, F. & Calfapietra, C. Neighborhood-scale reductions in heatwave burden projected under a 30% minimum tree cover scenario. *npj Urban Sustain.* **5**, 50 (2025).
18. Meili, N. et al. Tree effects on urban microclimate: Diurnal, seasonal, and climatic temperature differences explained by separating radiation, evapotranspiration, and roughness effects. *Urban Forestry Urban Green.* **58**, 126970 (2021).
19. Park, Y., Zhao, Q., Guldmann, J.-M. & Wentz, E. A. Quantifying the cumulative cooling effects of 3D building and tree shade with high resolution thermal imagery in a hot arid urban climate. *Landsc. Urban Plan.* **240**, 104874 (2023).
20. Li, H. et al. Cooling efficacy of trees across cities is determined by background climate, urban morphology, and tree trait. *Commun. Earth Environ.* **5**, 754 (2024).
21. Tan, P. Y. et al. Transpiration and cooling potential of tropical urban trees from different native habitats. *Sci. Total Environ.* **705**, 135764 (2020).
22. Schwaab, J. et al. The role of urban trees in reducing land surface temperatures in European cities. *Nat. Commun.* **12**, 6763 (2021).
23. Kántor, N., Chen, L. & Gál, C. V. Human-biometeorological significance of shading in urban public spaces-Summertime measurements in Pécs, Hungary. *Landsc. Urban Plan.* **170**, 241–255 (2018).
24. Makaremi, N., Salleh, E., Jaafar, M. Z. & GhaffarianHoseini, A. Thermal comfort conditions of shaded outdoor spaces in hot and humid climate of Malaysia. *Build. Environ.* **48**, 7–14 (2012).
25. Johansson, E. & Emmanuel, R. The influence of urban design on outdoor thermal comfort in the hot, humid city of Colombo, Sri Lanka. *Int. J. Biometeorol.* **51**, 119–133 (2006).
26. Middel, A., AlKhaled, S., Schneider, F.A., Hagen, B., Coseo, P.: 50 Grades of Shade. *Bull. Am. Meteorol. Soc.* https://doi.org/10.1175/BAMS-D-20-0193.1 (2021).
27. Forests, A. American Forests Launches Nationwide Tree Equity Scores https://www.americanforests.org/article/american-forests-launches-nationwide-tree-equity-scores/ Accessed 2025-07-09 (2021).
28. Locke, D. H. et al. Residential housing segregation and urban tree canopy in 37 US Cities. *npj Urban Sustain.* **1**, 15 (2021).
29. Wu, S., Chen, B., Webster, C., Xu, B. & Gong, P. Improved human greenspace exposure equality during 21st century urbanization. *Nat. Commun.* **14**, 6460 (2023).
30. Bakhtsiyarava, M. et al. Potential drivers of urban green space availability in Latin American cities. *Nat. Cities* **1**, 842–852 (2024).
31. Yang, Z. & Peng, J. Efficiency-oriented phased urban green space planning framework to mitigate heat-stress exposure. *npj Urban Sustain.* **5**, 57 (2025).
32. Zhang, X. et al. A strong but uneven increase in urban tree cover in China over the recent decade. *Nat. Cities* **2**, 460–469 (2025).
33. McDonald, R. I. et al. Current inequality and future potential of US urban tree cover for reducing heat-related health impacts. *npj Urban Sustain.* **4**, 1–16 (2024).
34. Gai, Z. et al. How does shade infrastructure affect outdoor thermal comfort during hot, humid summers? Evidence from Nanjing, China. *Build. Environ.* **267**, 112320 (2025).
35. Speak, A., Montagnani, L., Wellstein, C. & Zerbe, S. The influence of tree traits on urban ground surface shade cooling. *Landsc. Urban Plan.* **197**, 103748 (2020).

36. Armson, D., Stringer, P. & Ennos, A. R. The effect of tree shade and grass on surface and globe temperatures in an urban area. *Urban Forestry Urban Green.* **11**, 245–255 (2012).
37. Georgescu, M., Broadbent, A. M. & Krayenhoff, E. S. Quantifying the decrease in heat exposure through adaptation and mitigation in twenty-first-century US cities. *Nat. Cities* **1**, 42–50 (2024).
38. Maged, A., Abdelalim, A. & Mohamed, A. F. A. Generative design optimization of tree distribution for enhanced thermal comfort in communal spaces with special reference to hot arid climates. *Sci. Rep.* **15**, 16659 (2025).
39. Chen, B. et al. Advancing urban shade mapping for planning: Integrating shade demand and greening potential. *Urban Forestry Urban Green.* **111**, 128888 (2025).
40. Bloch, S. Shade: The Promise of a Forgotten Natural Resource, New York (2025).
41. Beuster, L. et al. (Slim) Shady - The relative role of buildings and trees in urban shade provision for pedestrians. Research Square. ISSN: 2693-5015 https://doi.org/10.21203/rs.3.rs-6966874/v1. https://www.researchsquare.com/article/rs-6966874/v1 Accessed 2025-08-04 (2025).
42. Gu, X. & Zhang, J. Green and grey cooling: Mitigating pedestrians perceived temperature via urban shades. *Build. Environ.* **285**, 113585 (2025).
43. Endreny, T. A. Mapping inequities in green cooling services. *Nat. Cities* **1**, 396–397 (2024).
44. Li, Y. et al. Green spaces provide substantial but unequal urban cooling globally. *Nat. Commun.* **15**, 7108 (2024).
45. Wu, S., Chen, B., An, J., Lin, C. & Gong, P. The interplay of cloud cover and 3D urban structures reduces human access to sunlight. *Nat. Cities* **1**, 686–694 (2024).
46. Bloch, S., Sambunaris, V. Opinion | In a Hotter World, We Need to Get Over Our Fear of Shadows. The New York Times Chap. Opinion. Accessed 2025-08-04 (2025).
47. Leng, S., Sun, R., Yang, X. & Chen, L. Global inequities in population exposure to urban greenspaces increased amidst tree and nontree vegetation cover expansion. *Commun. Earth Environ.* **4**, 464 (2023).
48. Pellerey, V. & Giezen, M. More green but less just? Analyzing urban green spaces, participation, and environmental justice in Amsterdam. *J. Environ. Plan. Manag.* **0**, 1–35 (2024).
49. Basu, R. & Ferreira, J. Sustainable mobility in auto-dominated Metro Boston: Challenges and opportunities post-COVID-19. *Transp. Policy* **103**, 197–210 (2021).
50. Lusk, A. C., Silva Filho, D. F. & Dobbert, L. Pedestrian and cyclist preferences for tree locations by sidewalks and cycle tracks and associated benefits: Worldwide implications from a study in Boston, MA. *Cities* **106**, 102111 (2020).
51. Ribeiro, M.C. et al. 4. Dealing with Fragmentation and Road Effects in Highly Degraded and Heterogeneous Landscapes. In: Gheler-Costa, C., Lyra-Jorge, M.C., Martins Verdade, L. (eds.) Biodiversity in Agricultural Landscapes of Southeastern Brazil, pp. 43–64. De Gruyter Open, https://doi.org/10.1515/9783110480849-006. https://www.degruyter.com/document/doi/10.1515/9783110480849-006/html Accessed 2025-08-13 (2016).
52. Ozberkman, D., Van Selm, M., Venverloo, T., Beuster, L. Sun Blocked: Integrating Shade into Urban Climate Assessments https://doi.org/10.5194/icuc12-797. https://meetingorganizer.copernicus.org/ICUC12/ICUC12-797.html Accessed 2025-08-04 (2025).
53. Lindberg, F. et al. Urban Multi-scale Environmental Predictor (UMEP): An integrated tool for city-based climate services. *Environ. Model. Softw.* **99**, 70–87 (2018).
54. AHN: Actueel Hoogtebestand Nederland. Publisher: AHN https://www.ahn.nl/ Accessed 2025-11-10 (2023).
55. Konarska, J., Lindberg, F., Larsson, A., Thorsson, S. & Holmer, B. Transmissivity of solar radiation through crowns of single urban trees-application for outdoor thermal comfort modelling. *Theor. Appl. Climatol.* **117**, 363–376 (2014).
56. Beuster, L. KerbSide. original-date: 2024-12-24T07:04:07Z https://github.com/lukasbeuster/KerbSide Accessed 2025-08-04 (2025).
57. Liu, Y., Zhang, G. & Yang, W. Dynamic estimation of urban heat exposure for outdoor jogging: Combining individual trajectory and mean radiant temperature. *Urban Clim.* **55**, 101871 (2024).
58. Gu, X., Lai, Z., Zhu, L. & Liu, X. Urban greenery distribution and its heat mitigation effect on outdoor jogging activities. *Urban Forestry amp; Urban Green.* **104**, 128655 (2025).
59. Tu, Y. et al. Inequality in infrastructure access and its association with health disparities. Nature Human Behaviour, 1–14 https://doi.org/10.1038/s41562-025-02208-3. Publisher: Nature Publishing Group. Accessed 2025-05-25 (2025).
60. Department, O.E. Housing Markets, Wealth and the Business Cycle. OECD Economics Department Working Papers 394, OECD Economics Department https://doi.org/10.1787/534328100627. https://www.oecd.org/en/publications/housing-markets-wealth-and-the-business-cycle_534328100627.html Accessed 2025-11-04 (June 2004).
61. De Nadai, M., Lepri, B. The Economic Value of Neighborhoods: Predicting Real Estate Prices from the Urban Environment. In: 2018 IEEE 5th International Conference on Data Science and Advanced Analytics (DSAA), pp. 323–330. IEEE, Turin, Italy https://doi.org/10.1109/DSAA.2018.00043. https://ieeexplore.ieee.org/document/8631423/ Accessed 2025-11-04 (2018).
62. Hui, E. C. M., Chau, C. K., Pun, L. & Law, M. Y. Measuring the neighboring and environmental effects on residential property value: Using spatial weighting matrix. *Build. Environ.* **42**, 2333–2343 (2007).
63. Kamath, H. G. et al. GLObal Building heights for Urban Studies (UT-GLOBUS) for city- and street- scale urban simulations: Development and first applications. *Sci. Data* **11**, 886 (2024).
64. Tolan, J. et al. Very high resolution canopy height maps from RGB imagery using self-supervised vision transformer and convolutional decoder trained on aerial lidar. *Remote Sens. Environ.* **300**, 113888 (2024).
65. Potapov, P. et al. The Global 2000-2020 Land Cover and Land Use Change Dataset Derived From the Landsat Archive: First Results. *Front. Remote Sens.* **3**, https://doi.org/10.3389/frsen.2022.856903. Publisher: Frontiers. Accessed 2025-08-04 (2022).
66. Che, Y. et al. 3D-GloBFP: the first global three-dimensional building footprint dataset. *Earth Syst. Sci. Data* **16**, 5357–5374 (2024).
67. Chen, T., Guestrin, C. XGBoost: A Scalable Tree Boosting System. In: Proceedings of the 22nd ACM SIGKDD International Conference on Knowledge Discovery And Data Mining, pp. 785–794. ACM, San Francisco California USA https://doi.org/10.1145/2939672.2939785. Accessed 2025-07-02 (2016).
68. Gu, X., Wu, Z., Liu, X., Qiao, R. & Jiang, Q. Exploring the Nonlinear Interplay between Urban Morphology and Nighttime Thermal Environment. *Sustain. Cities Soc.* **101**, 105176 (2024).
69. Lundberg, S., Lee, S.-I. A unified approach to interpreting model predictions. arXiv. arXiv:1705.07874 [cs] version: **1** https://doi.org/10.48550/arXiv.1705.07874. http://arxiv.org/abs/1705.07874 Accessed 2025-08-04 (2017).

Acknowledgements

The authors would like to thank the AMS Institute; all members of the MIT Senseable City Consortium (including Dubai Future Foundation, Abu Dhabi's Department of Municipalities and Transport, Atlas University, City of Laval, City of Rio de Janeiro, Consiglio per la Ricerca in Agricoltura e l'Analisi dell'Economia Agraria, FAE Technology, Hospital Israelita Albert Einstein, Sondotécnica, Toyota, Volkswagen Group America); Research Institute for Land and Space (RILS), The Hong Kong Polytechnic University (CDL1); and RGC Research Impact Fund (PolyU as PC) (R5011-23) for supporting this research.

Author contributions

X.G., L.B., T.V., and F.D. conceptualised and co-designed the experiments. X.G. and L.B. curated the data and performed the analysis. X.G., L.B., T.V., F.D., E.L., and X.L. discussed the design, methods, and results. X.L., T.V., and F.D. acquired funding and supervised the project. X.G. and L.B. wrote the original draft. X.G., L.B., T.V., F.D., E.L., and X.L. reviewed and edited the manuscript.

Competing interests

The authors declare no competing interests.

Additional information

Supplementary information The online version contains supplementary material available at https://doi.org/10.1038/s41467-026-69190-w.

Correspondence and requests for materials should be addressed to Xinyue Gu, Xintao Liu or Fábio Duarte.

Peer review information *Nature Communications* thanks the anonymous reviewer(s) for their contribution to the peer review of this work. A peer review file is available.